

# Structure and Magnetic Order in the NdFeAsO<sub>1-x</sub>F<sub>x</sub> Superconductor System

Y. Qiu,<sup>1,2</sup> Wei Bao,<sup>3,\*</sup> Q. Huang,<sup>1</sup> T. Yildirim,<sup>1</sup> J. M. Simmons,<sup>1,2</sup> M. A. Green,<sup>1,2</sup>  
J.W. Lynn,<sup>1</sup> Y.C. Gasparovic,<sup>1,2</sup> J. Li,<sup>1,2</sup> T. Wu,<sup>4</sup> G. Wu,<sup>4</sup> and X.H. Chen<sup>4</sup>

<sup>1</sup>*NIST Center for Neutron Research, National Institute of Standards and Technology, Gaithersburg, MD 20899, USA*

<sup>2</sup>*Department of Materials Science and Engineering,  
University of Maryland, College Park, MD 20742, USA*

<sup>3</sup>*Los Alamos National Laboratory, Los Alamos, NM 87545, USA*

<sup>4</sup>*Hefei National Laboratory for Physical Science at Microscale and Department of Physics,  
University of Science and Technology of China, Hefei, Anhui 230026, China*

The transition temperature  $T_C \approx 26$  K of the recently discovered superconductor LaFeAsO<sub>1-x</sub>F<sub>x</sub>[1] has been demonstrated to be extremely sensitive to the lanthanide ion, reaching 55 K for the Sm containing oxypnictides[2, 3, 4, 5, 6, 7, 8, 9, 10]. Therefore, it is important to determine how the moment on the lanthanide affects the overall magnetism in these systems. Here we report a neutron diffraction study of the Nd oxypnictides. Long ranged antiferromagnetic order is apparent in NdFeAsO below 1.96 K. Rietveld refinement shows that both Fe and Nd magnetic ordering are required to describe the observed data with the staggered moment 1.55(4)  $\mu_B$ /Nd and 0.9(1)  $\mu_B$ /Fe at 0.3 K. The other structural properties such as the tetragonal-orthorhombic distortion are found to be very similar to those in LaFeAsO. Neither the magnetic ordering nor the structural distortion occur in the superconducting sample NdFeAsO<sub>0.80</sub>F<sub>0.20</sub> at any temperatures down to 1.5 K.

PACS numbers: 74.25.Ha,74.70.-b,75.30.Fv,61.05.fm

The surprising discovery of high  $T_C$  superconductivity in cuprates two decades ago has shifted attention to laminar magnetic materials for new high  $T_C$  superconductors. New superconductors have been discovered since then in layered ruthenate[11] and triangular materials[12, 13, 14]. While these discoveries broke new ground for physics, their  $T_C$ 's are not high. The recent discovery of high  $T_C$  superconductors in the quaternary Fe oxypnictides LnFeAsO<sub>1-x</sub>F<sub>x</sub> has revitalized the field, and the question naturally arises as to how the new family of iron-based superconductors compare to the cuprates. Parent compounds of the new superconductors share a similar electronic structure with all five  $d$ -orbitals of the Fe contributing to a low density of states at the Fermi level[15, 16, 17, 18, 19, 20, 21, 22]. This contrasts with cuprates in which parent compounds are Mott insulators with well defined local magnetic moments[23]. On the other hand, the electron and hole doping phase diagram of the Fe oxypnictide systems[1, 7, 24, 25] is remarkably similar to that of the cuprates, for which the high- $T_C$  superconductivity occurs when the antiferromagnetic order of the parent compounds is suppressed by doping. This similarity has inspired a flurry of theoretical and experimental works.

A common phase diagram for these compounds has emerged in which the stoichiometric parent compound shows a structural anomaly around 150 K, below which spin-density-wave (SDW) antiferromagnetic ordering[15] appears, which is due to nesting Fermi surfaces that are dominated by electronic states of Fe[16]. This SDW ordering is shown to break the degeneracy between the  $d_{xz}$  and  $d_{yz}$  orbitals of the Fe ion, consistent with the observed tetragonal-orthorhombic structural distortion[22].

Superconductivity only occurs when this anomaly is suppressed, which can be achieved in a number of ways such as fluorine doping on the oxygen site[1, 7, 24, 25]. Despite these common features, a wider picture as to how the moment on the lanthanide affects the overall magnetism or why the superconducting transition temperature varies so greatly with different lanthanide ions is still unclear. So far, the magnetic structure has been determined only for LaFeAsO in a system without magnetic rare-earth elements[26]. Thus, it is instrumental to establish whether or not this is a general feature of the LnFeAsO<sub>1-x</sub>F<sub>x</sub> systems.

The NdFeAsO<sub>1-x</sub>F<sub>x</sub> system is the first one to have  $T_C \geq 50$  K[4] and now shares the honor with the Ln=Pr, Sm, and Gd compounds[6, 7, 8, 10]. In this study, we choose NdFeAsO to represent the non-superconducting members of the system, and NdFeAsO<sub>0.80</sub>F<sub>0.20</sub> the superconducting ones. Polycrystalline samples of 2.6 g NdFeAsO and 7.6 g NdFeAsO<sub>0.80</sub>F<sub>0.20</sub> were synthesized using the solid state reaction. We measured resistivity of both samples using the standard four-probe method from pieces from the same batch of samples synthesized for neutron diffraction experiments. The NdFeAsO sample shows a strong anomaly at  $T_S \sim 150$  K (Figure 1), slightly higher than the previously reported value of  $\sim 145$  K[25], which testifies to the good sample stoichiometry since  $T_S$  is known to decrease with doping[25]. The superconducting transition temperature of the NdFeAsO<sub>0.80</sub>F<sub>0.20</sub> sample is  $T_C \approx 50$  K.

Like in LaFeAsO, the resistivity anomaly is associated with a structure transition at  $T_S$ . Powder diffraction spectra of NdFeAsO measured at 175 and 4 K with neutrons of wavelength  $\lambda = 2.079\text{\AA}$ , using the high reso-

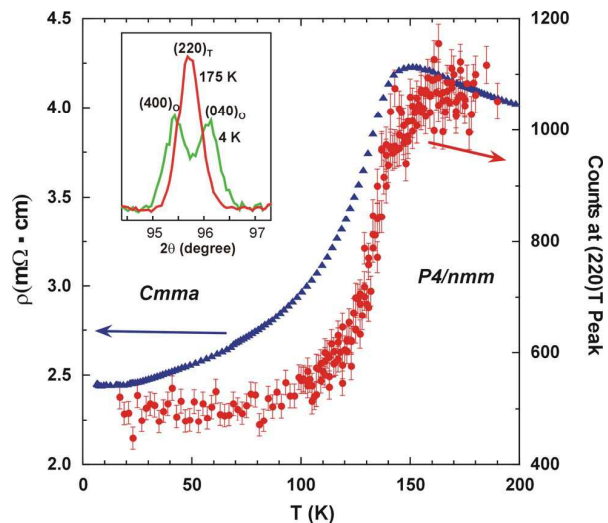


FIG. 1: (color online) Structural transition and its accompanying anomaly in resistivity in NdFeAsO. Both occur at  $T_S \approx 150$  K. Above the transition, the crystal has the tetragonal  $P4/nmm$  symmetry. Below  $T_S$ , the crystal is distorted to have the orthorhombic  $Cmma$  symmetry. The transition splits the tetragonal  $(220)_T$  Bragg peak into orthorhombic  $(400)_O$  and  $(040)_O$  peaks as shown in the inset.

lution powder diffractometer BT1 at the NIST Center for Neutron Research (NCNR), are shown in Fig. 2(a) and (b) together with the refined profiles using the GSAS program[27]. The high temperature structure is well described by the tetragonal ZrCuSiAs structure and the structure parameters at 175 K using space group  $P4/nmm$  are listed in Table 1. Only small amounts of impurity phases, 1.5% of Fe and less than 1% of other impurities, were present in our NdFeAsO sample. The occupancy of all sites are within one standard deviation of the NdFeAsO sample stoichiometry, therefore, the final refinement was performed with the fixed stoichiometric occupancy. Below  $T_S$ , NdFeAsO experiences an orthorhombic distortion. The low temperature structure is well accounted for by the space group  $Cmma$  and the refinement at 4 K is shown in Fig. 2(b).

The orthorhombic distortion doubles the unit cell, which is approximately  $(\sqrt{2}a + \varepsilon) \times (\sqrt{2}a - \varepsilon) \times c$  in terms of the tetragonal unit cell. This splits the  $(220)_T$  Bragg peak of the tetragonal structure into nonequivalent  $(400)_O$  and  $(040)_O$  Bragg peaks of the orthorhombic structure, see inset to Fig. 1. In terms of primitive cell parameters (Table 1), the distorted structure has  $\gamma = 90.296^\circ$ , which is almost identical to that of LaFeAsO[26], indicating Nd has almost no effect on the structural distortion. This is consistent with a recent theoretical study where it was shown that the structural distortion is due to the ordering of the Fe  $d_{xz}, d_{yz}$  orbitals in the SDW structure[22]. To establish the relation between the structural transition and the resistivity anomaly for

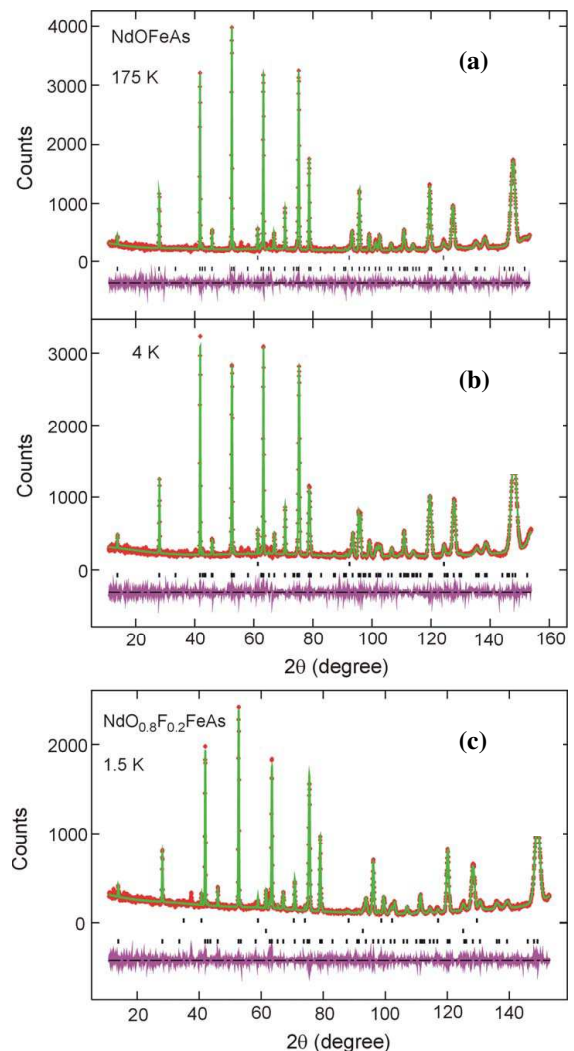


FIG. 2: (color online) Neutron powder diffraction spectra of NdFeAsO at (a) 175 and (b) 4 K, and (c) of NdFeAsO<sub>0.80</sub>F<sub>0.20</sub> at 1.5 K. While the spectra in (a) and (c) were refined by the space group  $P4/nmm$ , the spectrum in (b) was by the space group  $Cmma$ .

NdFeAsO, the intensity at the peak position of  $(220)_T$  was measured as a function of temperature. As shown in Fig. 1, it is obvious that the anomaly in resistivity is caused by the structural phase transition at  $T_S \approx 150$  K, like previously discovered in LaFeAsO[26].

There is no structural transition in our superconducting NdFeAsO<sub>0.80</sub>F<sub>0.20</sub> sample. The tetragonal ZrCuSiAs structure well describes the observed powder diffraction spectra down to 1.5 K. Fig. 2(c) shows the spectrum at 1.5 K together with the refined profile. Only small amounts of impurity phases, 1.5% of Fe and 4.4% of NdAs, were present in the sample. Refined structure parameters at 1.5 are listed in Table 1. The lattice of the NdFeAsO<sub>1-x</sub>F<sub>x</sub> system is more compact than that of the LaFeAsO<sub>1-x</sub>F<sub>x</sub> system[26, 28], and the  $T_C$  of the

TABLE I: Refined structure parameters for NdFeAsO at 0.3 K and 175 K and NdFeAsO<sub>0.8</sub>F<sub>0.2</sub> at 1.5K, respectively. Note that for the low-temperature structure of NdFeAsO, we also give the  $\gamma$  angle for the primitive cell of the Cmma space group, which is about the same as that of LaFeAsO. Similarly, the Fe-As distance is 2.40 Å for both Nd and La compounds. The As-Fe-As angles are 111.2° and 108.82° for NdFeAsO while the corresponding angles in LaFeAsO are 113.99° and 107.06°, respectively. It seems that the closer the As-Fe-As angle is to the ideal tetrahedral-angle  $\arccos(-\frac{1}{3}) = 109.47^\circ$ , the higher the  $T_C$ .

NdFeAsO at 0.3 K								NdFeAsO at 175 K				NdFeAsO <sub>0.8</sub> F <sub>0.2</sub> at 1.5 K						
Space Group: Cmma								Space Group: P4/nmm				Space Group: P4/nmm						
a=5.6159(1) Å, b=5.5870(1) Å, c=8.5570(2) Å								a=b=3.9611(1) Å,				a=b=3.9495(1) Å						
V=268.49 Å <sup>3</sup> (Prim. Cell: a=b=3.9608 Å, $\gamma = 90.296^\circ$ )								c=8.5724(2) Å, V=134.51 Å <sup>3</sup>				c=8.5370(3) Å, V=133.16 Å <sup>3</sup>						
$R_p = 3.62\%$ , $wR_p = 4.86\%$ , $\chi^2 = 1.511$								$R_p = 4.95\%$ , $wR_p = 6.46\%$				$R_p = 5.74\%$ , $wR_p = 7.72\%$						
Atom	site	x	y	z	B(Å <sup>2</sup> )	$M_x(\mu_B)$	$M_z(\mu_B)$	M( $\mu_B$ )	site	x	y	z	B(Å <sup>2</sup> )	site	x	y	z	B(Å <sup>2</sup> )
Nd	4g	0	$\frac{1}{4}$	0.1389(2)	0.06(5)	1.22(7)	0.96(9)	1.55(4)	2c	$\frac{1}{4}$	$\frac{1}{4}$	0.1393(3)	0.29(6)	2c	$\frac{1}{4}$	$\frac{1}{4}$	0.1421(4)	0.54(5)
Fe	4b	$\frac{1}{4}$	0	$\frac{1}{2}$	0.68(4)	0.9(1)	0	0.9(1)	2b	$\frac{3}{4}$	$\frac{1}{4}$	$\frac{1}{2}$	0.61(5)	2b	$\frac{3}{4}$	$\frac{1}{4}$	$\frac{1}{2}$	0.12(4)
As	4g	0	$\frac{1}{4}$	0.6584(4)	0.97(8)				2c	$\frac{1}{4}$	$\frac{3}{4}$	0.6580(4)	1.00(8)	2c	$\frac{1}{4}$	$\frac{3}{4}$	0.6599(4)	0.54(5)
O/F	4a	$\frac{1}{4}$	0	0	0.56(9)				2a	$\frac{3}{4}$	$\frac{1}{4}$	0	0.68(7)	2a	$\frac{3}{4}$	$\frac{1}{4}$	0	0.12(4)

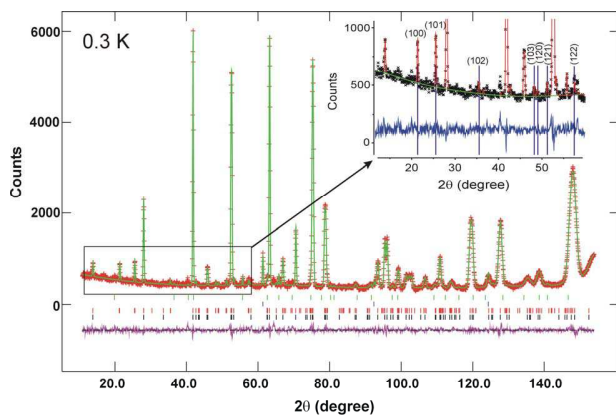


FIG. 3: (color online) Neutron powder diffraction spectrum at 0.3 K. The small angle part is magnified in the inset, and magnetic Bragg peaks which are absent at 4 K are marked by the vertical lines and are indexed using the orthorhombic *Cmma* unit cell.

former is higher than  $T_C$  of the latter. However, the structural transition temperature  $T_S$  of the two systems remains the same.

Despite the similarity with the structural transition in NdFeAsO and LaFeAsO, we did not observe the SDW order of the type observed in LaFeAsO with the magnetic wavevector  $(1/2, 1/2, 1/2)_T$  [26] in either our NdFeAsO sample down to 1.5 K or the NdFeAsO<sub>0.80</sub>F<sub>0.20</sub> sample down to 6 K, using BT1 or higher flux triple-axis spectrometer BT9 or BT7 at the NCNR. Our measurements at BT9 and BT7 set the upper limit for the staggered magnetic moment of the LaFeAsO-like SDW order at below 0.17  $\mu_B$  per Fe at 30 K for NdFeAsO and below 0.08  $\mu_B$  per Fe at 45 K for NdFeAsO<sub>0.80</sub>F<sub>0.20</sub>. However, the long ranged magnetic order is apparent below 2 K. In Fig. 3, neutron powder diffraction spectrum measured at BT1 at 0.3 K for the NdFeAsO sample in a <sup>3</sup>He cryostat is shown. When compared to the spectrum taken at

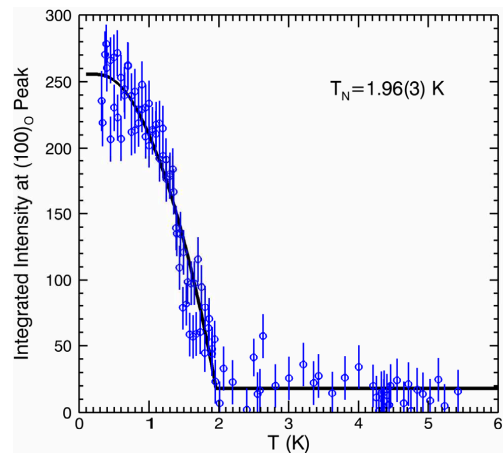


FIG. 4: (color online) The intensity of magnetic Bragg peak  $(100)_O$  as a function of temperature.

4 K in Fig. 2(b), additional magnetic Bragg reflections are visible and marked by the vertical lines in the inset. In Fig. 4, the temperature dependence of the magnetic Bragg peak  $(100)_O$ , measured at BT7, is shown. The solid line represents the mean-field theoretical fit for the squared magnetic order-parameter and the Néel temperature is determined as  $T_N = 1.96(3)$  K.

The magnetic wave-vector  $(1/2, 1/2, 0)_T$  of the low temperature antiferromagnetic order in NdFeAsO is consistent with the orthorhombic crystal structure below  $T_S$ . Therefore, there is no further crystal symmetry breaking below  $T_N$ . The parallel alignment of magnetic moments along the *c*-axis demanded by the magnetic wave-vector in NdFeAsO differs from the antiferromagnetic one in LaFeAsO, which further doubles the unit cell along the *c*-axis. The low  $T_N = 1.96(3)$  K indicates the important role played by Nd in the antiferromagnetic transition, as rare-earth magnetic ions often order at low temperature, such as in the high  $T_C$  cuprate Nd<sub>2-x</sub>Ce<sub>x</sub>CuO<sub>4</sub> system

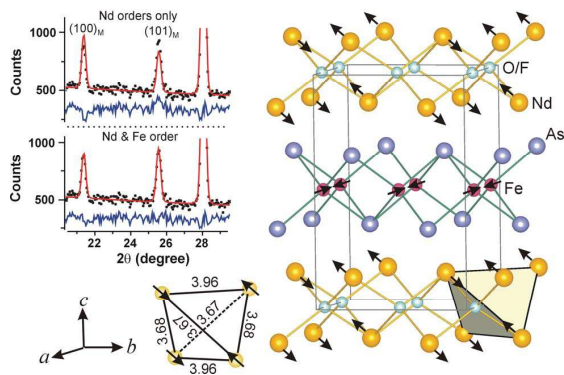


FIG. 5: (color online) Magnetic structure of NdFeAsO below  $T_N = 1.96$  K in the orthorhombic unit cell. The Nd tetrahedron structure element is also shown. A comparison of the Rietveld refinement fits using a Nd only model as compared with a Nd/Fe coupled model is included to highlight the necessity for the latter to fully describe the scattering.

below  $\sim 1.2$  K[29, 30]. However, a magnetic model with Nd ions alone cannot account for the magnetic diffraction pattern, see Fig. 5. We solved the magnetic order using a combined Nd and Fe antiferromagnetic structure. Comparison of the Rietveld refinement fits to magnetic models with different moment directions and the directions of the ferro and antiferro-alignment of the moments clearly shows significantly better result for the model shown in Fig. 5. The resulting crystalline and magnetic refinement is shown in Fig. 3 and the structure and magnetic parameters at 0.3 K are listed in Table 1. The Fe moments are orientated along the longer of the two axis,  $a$ , the direction where Nd also has a component. While the antiferromagnetic alignment for Nd is along the  $b$ -axis, it is along the  $a$ -axis for the Fe moments, consistent with previous first-principles calculations[22]. The total staggered magnetic moments are  $1.55(4) \mu_B$  per Nd and  $0.9(1) \mu_B$  per Fe at 0.3 K.

In conclusion, we presented a detailed study of the structural and magnetic properties of NdFeAsO and the doped 50 K superconductor NdFeAsO $_{0.80}$ F $_{0.20}$ . We clearly show that NdFeAsO has very similar structural properties to LaFeAsO system, and the main differences show up at very low temperatures where the Nd and Fe moments are ordered. We were not able to observe the Fe SDW ordering, suggesting that the Fe moment in NdFeAsO should be much smaller than that in LaFeAsO. In fact, all-electron first-principles calculations, similar to one in Ref. [22] but using the LaFeAsO structure with the lattice parameters of NdFeAsO, show that the Fe moment is reduced from  $0.48\mu_B$  for La to  $0.30\mu_B$  for Nd. Since the Bragg intensity is proportional to the square of the ordered moment, this suggests about 1/3 intensity decrease in NdFeAsO compared to the La-system, providing a possible explanation why we did not observe the Fe SDW ordering in NdFeAsO. From our results, it

is tempting to conclude that the reason for the higher  $T_c$  in NdFeAsO is the different structure parameters due to smaller lanthanide ion (Table I) and not due to other effects.

Work at LANL is supported by U.S. DOE, at USTC by the Natural Science Foundation of China, Ministry of Science and Technology of China (973 Project No: 2006CB601001) and by National Basic Research Program of China (2006CB922005).

Note added: After the completion of our work, an independent neutron diffraction study on NdFeAsO $_{1-x}$ F $_x$  was posted[31]. Consistent with our observations, Bos et al. also only observed magnetic transition at very low temperature. However, they did not determine the Néel temperature, and their conclusion of the antiferromagnetic order formed by the Nd moments alone has been shown in our work as inadequate.

---

\* Electronic address: wbao@lanl.gov

- [1] Y. Kamihara et al., J. Am. Chem. Soc. **130**, 3296 (2008).
- [2] X. H. Chen et al., Nature **453**, 761 (2008).
- [3] G. F. Chen et al., Phys. Rev. Lett. **100**, 247002 (2008).
- [4] Z. A. Ren et al., Europhys. Lett. **82**, 57002 (2008).
- [5] Z. A. Ren et al., arXiv:0803.4283 (2008).
- [6] Z. A. Ren et al., Chinese Phys. Lett. **25**, 2215 (2008).
- [7] R. H. Liu et al., arXiv:0804.2105 (2008).
- [8] Z.-A. Ren et al., arXiv:0804.2582 (2008).
- [9] Z. A. Ren et al., Supercond. Sci. Technol. **21**, 082001 (2008).
- [10] C. Wang et al., arXiv:0804.4290 (2008).
- [11] Y. Maeno, H. Hashimoto, K. Yoshida, S. Nishizaki, T. Fujita, J. G. Bednorz, and F. Lichtenberg, Nature **372**, 532 (1994).
- [12] M. J. Geselbracht et al., Nature **345**, 324 (1990).
- [13] K. Takada et al., Nature **422**, 53 (2003).
- [14] E. Morosan et al., Nature Phys. **2**, 544 (2006).
- [15] J. Dong et al., arXiv:0803.3426 (Europhys. Lett. in-press) (2008).
- [16] D. J. Singh and M.-H. Du, Phys. Rev. Lett. **100**, 237003 (2008).
- [17] S. Lebegue, Phys. Rev. B **75**, 035110 (2007).
- [18] K. Haule et al., Phys. Rev. Lett. **100**, 226402 (2008).
- [19] C. Cao et al., arXiv:0803.3236 (2008).
- [20] F. Ma and Z. Y. Lu, arXiv:0803.3286 (2008).
- [21] I. A. Nekrasov et al., arXiv:0804.1239 (2008).
- [22] T. Yildirim, arXiv:0804.2252 (Phys. Rev. Lett. in press) (2008).
- [23] P. W. Anderson, Science **235**, 1196 (1987).
- [24] H. H. Wen et al., Europhys. Lett. **82**, 17009 (2008).
- [25] G. F. Chen et al., Chinese Phys. Lett. **25**, 2235 (2008).
- [26] C. Cruz et al., Nature **453**, 899 (2008).
- [27] A. Larson and R.B. Von Dreele, *GSAS: Generalized Structure Analysis System*, (1994).
- [28] Y. Qiu et al., arXiv:0804.1062 (2008).
- [29] J. W. Lynn et al., Phys. Rev. B **41**, 2569 (1990).
- [30] R. Sachidanandam et al., Phys. Rev. B **56**, 260 (1997).
- [31] J.-W. G. Bos et al., arXiv:0806.1450 (2008).